- 1 Study of UV-Vis Molar Absorptivity Variation and Quantitation of Anthocyanins Using
- 2 Molar Relative Response Factor
- 3 Wen Dong^{1,2}, Xin Yang², Ning Zhang³, Pei Chen^{4,*}, Jianghao Sun⁴, James M. Harnly⁴, and
- 4 Mengliang Zhang^{1,*}
- ¹Department of Chemistry, Middle Tennessee State University, Murfreesboro, TN, 37132
- 6 ²Department of Computer Science, Middle Tennessee State University, Murfreesboro, TN,
- 7 37132
- 8 ³Department of Mathematics and Computer Science, Fisk University, Nashville, TN, 37208
- 9 ⁴Methods and Application of Food Composition Laboratory, Beltsville Human Nutrition
- 10 Research Center, Agricultural Research Service, United States Department of Agriculture,
- 11 Beltsville, MD, 20705
- 12

- 14 Email:
- Wen DONG, wen.dong@mtsu.edu
- 16 Xin YANG, <u>xin.yang@mtsu.edu</u>
- 17 Ning ZHANG, <u>nzhang@fisk.edu</u>
- 18 Pei CHEN, pei.chen@usda.gov
- 19 Jianghao SUN, Jianghao.sun@usda.gov
- James M. HARNLY, james.harnly@usda.gov
- 21 Mengliang ZHANG, <u>mzhang@mtsu.edu</u>

^{*}Corresponding authors: Mengliang Zhang, *E-mail address:* mzhang@mtsu.edu. Phone: +01 615-904-8439; Pei Chen, *E-mail address:* pei.chen@usda.gov. Phone: +1-301-504-8144.

Abstract

22

23

24

25

26

27

28

29

30

31

32

33

34

35

The effects of anthocyanin's substitution groups on the UV-Vis molar absorptivity were examined by analyzing a group of 31 anthocyanidin/anthocyanin reference standards with ultra-high performance liquid chromatography-diode array detector (UHPLC-DAD). The substitution groups on aglycones were found to associate with molar absorptivity variations, often neglected in anthocyanin quantitation, resulting in significant analytical errors. A simple yet comprehensive strategy based on the molar relative response factors (MRRFs) and a single master reference calibration (i.e., cyanidin-3-glucoside) was proposed to quantify anthocyanins in red cabbage, blueberry, and strawberry samples with improved analytical accuracy. The results indicate this approach provides an effective, inexpensive, and accurate analytical method for anthocyanins in food materials without using individual reference standards. MRRFs of 617 anthocyanins/anthocyanidins were calculated, and the information is freely available at https://BotanicalDC.online/anthocyanin/. This study could be critical to developing new reference methods for anthocyanin analysis and harmonizing results and data from various sources.

36

Keywords: Anthocyanins, quantitation, food, LC/UV, MRRF.

38 39

37

40 41

42 43

44

45 46

47 48

49

50 51

Abbreviations

53 54 55

56

57

58

59

60

61

62

63

64

65

66

67

68

69

70

Cy, cyanidin; MAPK, mitogen-activated protein kinase; EGFR, epidermal growth factor receptor; cAMP, cyclic adenosine monophosphate; PDEs, phosphodiesterases; HPLC, high-performance liquid chromatography; MS, mass spectrometry; MS/MS, tandem mass spectrometry; C3G, cyanidin-3-glucoside; M3G, malvidin-3-glucoside; λ_{max}, absorbance maxima; MRRFs, molar relative response factors; FA, formic acid; MeOH, methanol; ACN, acetonitrile; DAD, diode array detector; ESI, electrospray ionization; MS, mass spectrometry; UAE, extraction; C35G, cyanidin-3,5-di-O-glucoside; Cy-3-sam-5-glc, cyanidin-3-O-sambubioside-5-O-glucoside; Gp, gossypetinidin; Pg, pelargonidin; Ln, luteolinidin; Mv, malvidin; Ag, apigeninidin; Pt, petunidin; Dp-3-sam, delphinidin-3-O-sambubioside; D3G, delphinidin -3-Oglucoside; Dp, delphinidin; Dp-3-sam-5-glc, delphinidin-3-O-sambubioside-5-O-glucoside; D35G, delphinidin-3,5-di-O-glucoside; Pn, peonidin; λ_{acyl}, acylation absorbance maximum; MRRF_p, predicted MRRFs under λ_{max} ; MRRF_{C3G} 512, MRRFs with C3G reference under 512 nm; Fn, fisetinidin; Rn, robinetinidin; P3G, pelargonidin-3-O-glucoside; P35G, pelargonidin-3,5-di-Oglucoside; Dm, diosmetinidin; HCA, hydroxycinnamic acid; sin, sinapoyl; caf, caffeoyl; fer, feruloyl; cou, coumaroyl; phb, p-hydroxybenzoyl.

71 1. Introduction

72

73

74

75

76

77

78

79

80

81

82

83

84

85

86

87

88

89

90

91

92

93

Anthocyanins (of the Greek anthos = flower and kianos = blue) are a class of water-soluble natural flavonoids and secondary metabolites of plants that render them vivid red to blue (Khoo, Azlan, Tang & Lim, 2017). Anthocyanins are abundant in many color-intense fruits and vegetables, such as berries, beets, grapes, and purple potatoes (Chen, Su, Xu, Bao & Zheng, 2016, Han, Yang, Wang, Fernandes, Mateus & Liu, 2019, Jokioja et al., 2020), and they became attractive in the modern food industry due to their intensive colors and associated health-promoting benefits, including anti-oxidation, anti-cancer, and anti-diabetic (Gowd, Jia & Chen, 2017). Anthocyanins are glycosylated derivatives from anthocyanidins (aglycones), which consist of a core structure of hydroxyl-2-phenylbenzo-pyran cation and differ in the numbers and positions of hydroxyl and/or methoxy groups attached (Figure S1) (Cai et al., 2022). The type, number, and position of glycosyl attachments to the anthocyanidins and aliphatic or aromatic acid modifications of sugar moieties diversified anthocyanin structures. To date, more than 700 anthocyanins have been identified with 31 different core structures, among which cyanidin (46%), delphinidin (11%), pelargonidin (11%), peonidin (11%), petunidin (6.4%), and malvidin (6.4%) core based anthocyanins are predominantly found in nature (92%) and widely studied (Castañeda-Oyando, Pacheco-Hernández, Páez-Hernández, Rodríguez & Galán-Vidal, 2009, Gowd, Jia & Chen, 2017, Houghton, Appelhagen & Martin, 2021). Natural anthocyanins can also be classified into four major classes based on the sugar substitution: 3-mono-, 3-bi-, 3,5-di-, and 3,7-di-glycosides, where the 3-mono-glycosides are most prevalent (Saha, Singh, Paul, Sarkar, Khan & Banerjee, 2020). Anthocyanins, due to their long chromophore of eight conjugated double bonds and a positive charge on the heterocyclic oxygen ring under acidic conditions, present a unique UV-Vis absorption profile with a maximum in the visible range between 465 nm and 550 nm and another

absorption in the range between 270 nm and 280 nm (He & Giusti, 2010). Therefore, anthocyanins have been analyzed by UV-Vis spectroscopy extensively (Saha, Singh, Paul, Sarkar, Khan & Banerjee, 2020), and pH-differential spectrophotometric measurement of total monomeric anthocyanins equivalent is still being widely used in the food industry and research (Lee, Durst, & Wrolstad, 2005). It was reported that anthocyanins with different aglycones and sugar moieties may differ in their bioavailability and potential health effects (Marko, Puppel, Tjaden, Jakobs & Pahlke, 2004, Wu, Cao & Prior, 2002). For instance, an *in vitro* study showed that cyanidin (Cy) and delphinidin (Dp) inhibited tumor cell growth by down-regulating mitogen-activated protein kinase (MAPK) cascade activity through epidermal growth factor receptor (EGFR), while anthocyanidins bearing methoxy residues (i.e., malvidin and peonidin) targeted on cAMP hydrolysis and thus works as an inhibitor of cAMP-specific phosphodiesterases (PDEs) instead (Marko, Puppel, Tjaden, Jakobs & Pahlke, 2004). Hence, accurate quantification of individual anthocyanins is critical to the quality assurance of the food products, evaluating the dietary intake levels, and studying the role of anthocyanins in health and nutrition (Balentine et al., 2015). Researchers often attempt to characterize and quantify anthocyanins with high-performance liquid chromatography (HPLC) with UV-Vis detector, mass spectrometry (MS), tandem mass spectrometry (MS/MS), or combined (Zhang, Z., Kou, Fugal & McLaughlin, 2004) (Castañeda-Ovando, Pacheco-Hernández, Páez-Hernández, Rodríguez & Galán-Vidal, 2009). However, the quantitation of anthocyanins is challenging due to their complex and similar chemical structures and large varieties. There are three HPLC-based strategies for anthocyanin quantification commonly employed: a). To measure the respective aglycones after the hydrolysis of anthocyanins with strong acids, which provides no information on glycoside substitution or other modification patterns (Merken, Merken & Beecher, 2001); b). To quantify all anthocyanin peaks by using one

94

95

96

97

98

99

100

101

102

103

104

105

106

107

108

109

110

111

112

113

114

115

reference standard, usually cyanidin-3-glucoside (C3G) or malvidin-3-glucoside (M3G), which could only predict equivalents of other anthocyanidins to the monosaccharide anthocyanin selected (Wu, Gu, Prior & McKay, 2004); c). To further modify strategy b by applying molecular weight correction factors to calculate the concentration of individual anthocyanins by one of their representative reference standards in the same classes (Chandra, Rana & Li, 2001, Wu, Beecher, Holden, Haytowitz, Gebhardt & Prior, 2006). Among the three, strategy c is considered the most accurate for estimating individual anthocyanin content in food. However, this strategy requires using six mixed anthocyanin standards (i.e., 3-O-β-glucosides of pelargonidin, cyanidin, peonidin, delphinidin, petunidin, and malvidin) to construct the calibration curves. Nevertheless, in all three strategies, the peak areas of anthocyanins in food materials and calibration samples were often integrated from the chromatograms under the same wavelength instead of absorbance maxima (λ_{max}) for individual anthocyanins. It assumes the molar absorptivity of the anthocyanins is unchanged if they share the same aglycone, regardless of the number, the location, and the nature of sugars bonded to the molecule and the number and type of aromatic or aliphatic acids linked to the sugar. This assumption is problematic because the glycosylation of anthocyanidins has been reported to result in a hypsochromic shift (blue shift) in the λ_{max} and the change of absorbance ratio at 440 nm to the λ_{max} (Saha, Singh, Paul, Sarkar, Khan & Banerjee, 2020), which indicates the significant impact on molar absorptivity due to the structural variations, although how it affects the molar absorptivity quantitatively and analytical accuracy is largely unknown.

117

118

119

120

121

122

123

124

125

126

127

128

129

130

131

132

133

134

135

136

137

138

139

Molar relative response factors (MRRFs) can be used to correct the differences in detector responses of similar chromophores as well as the effects of functional groups on the UV-Vis spectra and λ_{max} , and this approach has been applied to study several flavonoid subclasses, such as flavonois, flavones, flavanois, isoflavones, and flavanones (Lin & Harnly, 2012, Lin, Harnly,

Zhang, Fan & Chen, 2012). For instance, missing 5-OH of isoflavones lowered the MRRFs by 0.34 or 34% decrease of absorbance per mole, while missing 4'-OH on apigenin caused the almost complete loss of the Bond I (305-390 nm) peak absorption. The addition of 5'-OH to the flavanols and proanthocyanins drastically decreased MRRFs by 0.7 or 70% lower on their Bond II (230-300 nm) peak absorbance per mole. Glycosyl and/or methyl substitutions also affected the MRRFs of isoflavones, flavanones, and chalcones. The implementation of MRRFs compensates for the UV-Vis absorbance changes due to the substitutions and allows accurate and inexpensive quantitation of flavonoids in each class with a single master reference standard. However, MRRFs for anthocyanins have not been studied due to several key challenges. First, anthocyanins undergo transformations with changes in the pH and could exist in four structural forms: flavylium cation (red), anhydrous quinoidal base (blue), carbinol base (colorless), and chalcone (pale yellow) (Castañeda-Ovando, Pacheco-Hernández, Páez-Hernández, Rodríguez & Galán-Vidal, 2009, Sun, Cao, Bai, Liao & Hu, 2010). In addition, compared to other flavonoids, hydroxylation, glycosylation, and acylation of anthocyanins cause a more significant λ_{max} shift, making molar absorptivity evaluation more complicated and difficult to predict. Moreover, the commercial reference standards of the desired quality and purity are limited and often expensive. Furthermore, preparing standard anthocyanins from plant sources or chemical synthesis requires enormous time and effort.

140

141

142

143

144

145

146

147

148

149

150

151

152

153

154

155

156

157

158

159

160

161

162

The objectives of the present study were to (i) examine the effect of substitutions of anthocyanidins on the UV-Vis molar absorptivity and evaluate their impact on quantitative accuracy; (ii) calculate MRRFs based on the experimental data and provide guidance to predict MRRFs of other anthocyanins; and (iii) develop a single master reference calibration strategy to quantify anthocyanins and apply the approach to study anthocyanins in food materials.

2. Materials and Methods

2.1.Chemicals and materials

HPLC-grade formic acid (FA), methanol (MeOH), acetonitrile (ACN), and water were purchased from Fisher Scientific, Inc. (Fair Lawn, NJ, USA). Reference standards, including 12 anthocyanidins and 19 anthocyanins, were purchased from Extrasynthese (Genay, Cedex, France) (Table S1). Fresh strawberries, blueberries, and red cabbage were purchased from a local Walmart supermarket in Murfreesboro, TN, USA.

2.2.Preparation of standard solutions

Accurately weighted 1.00-2.00 mg of reference standards were measured on a microbalance with a precision of 0.5 μg (Mettler Toledo XPR6UD5, Columbus, OH, USA) before and after 18-hour lyophilization (FreeZone 2.5plus, Labconco Corp., Kansas City, MO, USA) to calculate the percentage of moisture. The moisture in all standards was found to be less than 5%. The standard powders were then prepared into 1.0 mg/mL stock solutions according to the previous report (Zhang, Z., Kou, Fugal & McLaughlin, 2004) with modifications. Anthocyanidins were dissolved in 2N HCl acidified MeOH (i.e., 17 mL of 37% concentrated HCl + 83 mL of MeOH), and anthocyanins dissolved in MeOH/water (80:10, ν/ν) with 10% FA. Individual standard solutions and mixture solutions with 5-16 anthocyanidins/anthocyanins were diluted from the stock solutions to 50 μg/mL and prepared with water/MeOH/FA (80:10:10, ν/ν). The mixed standard solutions were further diluted to form a series of standard solutions in the 0.25-20 μg/mL range.

2.3.UHPLC-DAD-MS detection

Analyses were performed on a Dionex UltiMateTM 3000 UHPLC system coupled with an Accela photodiode array detector (DAD) and a Thermo LTQ XL mass spectrometer (Thermo Scientific, San Jose, CA, USA). The autosampler was maintained at 10 °C. The separation was

carried out on a Waters Acquity UHPLC HSS T3 RP18 column (100 × 2.1mm i.d., 1.8 μm, 100 Å) with an UltraLine UHPLC In-Line Filter (RESTEK, Bellefonte, PA, USA) at a flow rate of 0.4 mL/min and a column temperature at 40 °C. Elution was performed using mobile phase A (0.5% FA in water, *ν/ν*) and B (ACN). The linear gradient started at 2% B, held for 2 min, ramped from 2 to 5% B at 5 min, held for 5 min, from 5 to 8% B at 25 min, held for 5 min, and from 8 to 30% B at 40min, from 30 to 90% B at 45 min, and held for an additional 5 min. The DAD was set at 510 nm to monitor the elution in real-time, and the full UV-Vis spectra were recorded from 200 to 800 nm at a 1 nm increment. Eluates were also monitored in the positive ionization mode of electrospray ionization (ESI) - ion trap MS. Major MS parameters were as follows: source heater temperature at 250 °C, sheath gas at 35 (arbitrary units), sweep gas at 15 (arbitrary units), spray voltage at 3.5 kV, tube lens at 60 V, and capillary temperature at 200 °C. The mass range was from *m/z* 100 to 1000.

Plant extract samples were also screened for the identification of anthocyanins by a Bruker Elute UHPLC connected to a Bruker Compact QTOF mass spectrometer using an electrospray ionization probe (Bruker, Bremen, Germany). The chromatographic conditions remained the same as in the aforementioned LC-DAD method. The data were acquired in the full scan mode (range of m/z 50–1500) in positive mode using the capillary voltage at 4.5 kV; nebulizer and drying gas (N₂) at 2.0 bar and 8.0 L/min, respectively; dry temperature of 220 °C. The MS/MS spectra were acquired in Auto MS/MS mode using collision energy between 20-50 eV for the top three precursor ions in m/z 300-1500. Internal calibration of the instrument was accomplished using a 10 mM sodium formate solution introduced to the ion source via a 20 μ L loop at the beginning of each analysis. The compounds were identified by comparing the fragmentation pattern and high-

- accurate mass spectra and searching against the database via MetaboScape 2023 (Bruker, Bremen,
- 209 Germany).
- 2.4. *Ultrasound-assisted extraction (UAE) of anthocyanins*
- Before use, all plants were ground in liquid nitrogen and freeze-dried (FreeZone 2.5plus,
- Labconco Corp., Kansas City, MO, USA). Each powdered sample (about 250 mg) was extracted
- with 5.00 mL of 10% FA acidified MeOH/water (60:40, v/v), vortexed at 2000 rpm for 1 min, and
- 214 then sonicated for 60 min with ice bath followed by centrifugation at 447 g (2500 rpm) for 15 min
- 215 (AllegraTM 64R Centrifuge, Beckman Coulter, Inc., Brea, CA, USA) (Lin, Sun, Chen & Harnly,
- 216 2011, Wang, Sun, Zhou, Qiu & Cui, 2020). The supernatant was filtered through a 13 mm (0.22
- 217 µm) PVDF syringe filter (VWR Scientific, Seattle, WA, USA) and then diluted at a 1:5 ratio with
- water/MeOH/FA (80:10:10, v/v/v) prior to injecting 10 μ L into the LC-DAD system.
- 2.5.Data processing and statistical analysis
- The DAD data were converted to text files from RAW files by the Xcalibur plug-in tool,
- 221 MSGet developed by the Kazusa DNA Research Institute (Kisarazu, Japan), which were then read
- into MATLAB R2021a (MathWorks Inc., Natick, MA, USA) using an in-house algorithm. Two
- 223 MATLAB functions (i.e., 'peakfit.m' and 'findpeaksG.m') provided by Dr. Tom O'Haver
- 224 (https://terpconnect.umd.edu/~toh/spectrum/InteractivePeakFitter.htm), were used to simulate
- selected UV-Vis spectra to an unconditioned Gaussian curve and detect chromatographic peaks
- for which the peak areas were integrated using the method published previously (Zhang, M., Sun
- 227 & Chen, 2017). Statistical analysis was performed using MATLAB and Microsoft Excel
- 228 (Microsoft Corp., Redmond, WA, USA).
- 229 3. Results and discussion
- 230 *3.1.Chromatographic condition optimization*

The chromatographic separation of anthocyanidins/anthocyanins was optimized starting from a published method (Grace, Xiong, Esposito, Ehlenfeldt & Lila, 2019) with minor modifications: 43-min water (FA 0.5%, v/v) and MeOH gradient at the flow rate of 0.4 mL/min on a Waters Acquity BEH reverse phase C18 column (1.7 μm, 2.1 × 50 mm). Several chromatographic parameters were evaluated to achieve the best separation, including mobile phase, column temperature, column type, flow rate, and solvent used to prepare the samples. Initially, the main challenge of the optimization was to retain the di-glycosylated anthocyanins such as cyanidin-3,5di-O-glucoside (C35G) and cyanidin-3-O-sambubioside-5-O-glucoside (Cy-3-sam-5-glc) due to their high polarities. Among all the parameters, it was found that the dissolving solvent was the most important factor for retaining the polar anthocyanins. Practically, it is widely recommended to avoid solvents with higher elution strength than the mobile phase to dissolve samples and standards because a stronger injection solvent can interfere with the interactions between the sample molecules and the stationary phase of the column, especially when large injection volumes are used (Keunchkarian, Reta, Romero & Castells, 2006). In our study, C35G in water/MeOH/FA (30.60.10, v/v/v) was found unretained on the two C18 columns tested regardless of mobile phase composition but was retained with elution at 15.32 min under the HPLC conditions in Section 2.3 when water/MeOH/FA (80:10:10, v/v/v) was used to dilute the solutions. A lower MeOH ratio would cause less solubility for some anthocyanidins, especially gossypetinidin (Gp), pelargonidin (Pg), luteolinidin (Ln), and malvidin (Mv). The concentration of FA (i.e., 5% or 10%) in the dissolving solvent had no effect on the separation. Therefore, water/MeOH/FA (80:10:10, v/v/v) was chosen as the solvent composition prior to the HPLC injection for both standards and plant extracts. A few additional parameter changes also contributed to the improved chromatographic separation. Replacing MeOH with ACN in the mobile phase resulted in sharper peaks in the

231

232

233

234

235

236

237

238

239

240

241

242

243

244

245

246

247

248

249

250

251

252

chromatogram for most of the anthocyanins. Changing the starting mobile phase gradient from 5% ACN to 2% ACN was essential to resolve the C35G and Cy-3-sam-5-glc on the chromatogram. The substitution of a longer column (i.e., Waters Acquity UPLC HSS T3 RP18 column, 100 × 2.1 mm i.d., 1.8 µm, 100 Å) further improved the separation. As detailed in Section 2.3, a 50-min gradient was employed in our study, and a better separation of anthocyanins could be achieved but would significantly increase the total run time for each analysis. Consequently, the 31 standards were grouped into three mixtures, and their chromatograms are shown in Figure 1. Notably, 10 out of 11 anthocyanidins were fully separated at 8%-30% ACN except for the coelution of apigeninidin (Ag) and petunidin (Pt) (i.e., retention time difference<0.2 min, Table S1). In general, the polarity of anthocyanidins/anthocyanins increases as more hydroxyl groups and/or glycosyl substitutions exist on aglycones, resulting in faster elution on a reversed-phase LC system. For example, 3-glycosylated anthocyanins were eluted in the window between 3,5-diglycosylated anthocyanins and anthocyanidins, mostly eluted during 8% acetonitrile holding time except for delphinidin-3-O-sambubioside (Dp-3-sam) and delphinidin-3-O-glucoside (D3G) which were eluted at 5%-8% acetonitrile. Diglycosylated delphinidins (Dp) such as delphinidin-3-Osambubioside-5-O-glucoside (Dp-3-sam-5-glc) and delphinidin-3,5-di-O-glucoside (D35G) were among the earliest eluted anthocyanins. The elution order of anthocyanins agreed with the results from previous studies (Chandra Singh, Probst, Price & Kelso, 2022, Trikas, Papi, Kyriakidis & Zachariadis, 2016).

254

255

256

257

258

259

260

261

262

263

264

265

266

267

268

269

270

271

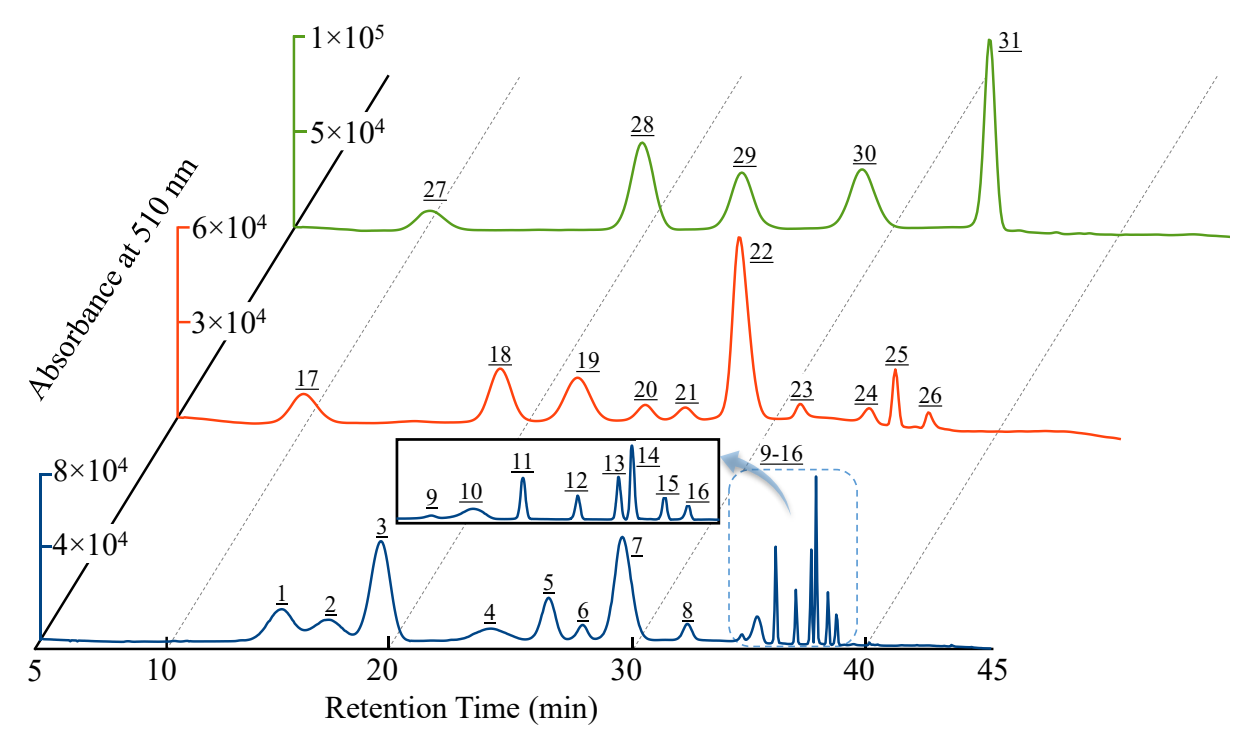


Figure 1. Chromatograms of 31 anthocyanidins and anthocyanins at 510 nm (A list of their chemical names and respective retention times is available in Table S1).

3.2. Stability of anthocyanins and anthocyanidins

The stability of anthocyanins is highly dependent on pH, as described earlier. It was reported that the form of anthocyanins dominated as flavylium cation on C-2 position at pH below 2.0, and it was fast hydrated, generating carbinol pseudobase or chalcone when the pH increased to 3.0 to 6.0 (Cai et al., 2022). A water/MeOH solution containing 10% FA (pH \approx 1.7) was used in this study to maintain the flavylium structures of anthocyanins. All the anthocyanin standards were tested stable for at least 24 h in this solution under 10 °C. Anthocyanidins, however, degraded in a range between 10% to 60% after 24 h with the same solution (Figure S2). The main product of the degradation was the hydrated anthocyanidins, resulting in the loss of absorbance at 510 nm and a much earlier retention time compared to its respective precursor anthocyanidins. The degradation products were further confirmed by the MS spectrum (Figure S2A). For instance, a hydrated product of Pt (m/z 335) was detected at a retention time of 30.0

min, which increased in peak height during the 24-h period. The degradation of six major anthocyanidins varies, as presented in Figure S2B. Pelargonidin and Mv were degraded slightly (<5%) in 24 h and nearly 10% after 48 h. Petunidin and peonidin (Pn) degraded at a similar extent: 30% in 24 h and 60% in 48 h. Cyanidin degraded 20% after 24 h and 40% after 48 h, whereas Dp was most unstable under this condition, degrading nearly 60% at 24 h and 80% at 48 h. The stability of flavylium cations is associated with the electron density of the aromatic center (Houghton, Appelhagen & Martin, 2021). The additional hydroxyl (-OH) groups in the B-ring decrease the stability due to the electronegativity of the oxygen atom, pulling electron density away from the electron-deficient flavylium structures. Our results agreed with this trend, providing stability of Pg > Cy > Dp as their B-rings with 1, 2, and 3 -OH groups, respectively. Electron donating groups such as methyl groups increase the electron density, thus enhancing stabilization. Therefore, Pn is more stable than Dp, and Mv is more stable than Pn due to the methylation of hydroxyl groups in the B-rings (Figure S2B). It was reported that a strong acidic environment (i.e., 2N HCl acidified MeOH) would improve the stability of anthocyanidins (Zhang, Z., Kou, Fugal & McLaughlin, 2004), and the stability of anthocyanidins in 2N HCl acidified MeOH for at least 24 h under 10 °C was also confirmed in our study. However, strong acidic conditions such as 2N HCl would hydrolyze anthocyanins into anthocyanidins. As a result, the stock solutions of anthocyanins and anthocyanidins were prepared in different solvents, water/MeOH/FA (80:10:10, v/v/v) and in 2N HCl acidified MeOH, respectively. It is worth noting that anthocyanidins rarely exist and are mostly found as anthocyanins in plants. However, it is important to investigate their stabilities in this study to ensure the accuracy of the MRRF measurement.

3.3.UV-Vis spectrum and MRRFs

286

287

288

289

290

291

292

293

294

295

296

297

298

299

300

301

302

303

304

305

306

307

The UV-Vis absorption of anthocyanins has been extensively studied. A typical UV-Vis spectrum of anthocyanin usually consists of two wavelength regions, 260-280 nm for the UV region and 490-550 nm for the visible region (Figure 2). Besides the two signature regions, anthocyanins could also present two humps in between that were used as an indicator of substitution groups. Generally, sugar substitutions give an absorption at 400–450 nm, the size of which was used to predict the number of sugars attached. Particularly, the absorbance ratio at 440 nm to the λ_{max} of 29-35% indicated the existence of one sugar moiety, while 15-24% indicated two sugar moieties. Such ratios would be two times higher when the glycosylation occurs at the 3-Oposition against the substitutions at position 5-O- or 3,5-O-. Another hump between 310–340 nm was usually observed whenever the sugar moiety was acylated, mostly on C3 sugars. The ratio of acylation maximum (λ_{acyl}) against visible maximum was found to be between 0.5 and 0.7 for single acylation and 0.8 and 1.1 for double acylations (Saha, Singh, Paul, Sarkar, Khan & Banerjee, 2020). For quantitative studies with the HPLC method, the absorption at one selected wavelength in the range of 510–520 nm is commonly recorded to monitor the anthocyanins' elution. However, the hydroxylation, methylation, and glycosylation on aglycones could cause λ_{max} shift, which was often not taken into consideration when calculating the anthocyanin concentrations and thus compromised the quantitative accuracy by failing to account for the change in the molar absorptivity due to the shift of λ_{max} .

309

310

311

312

313

314

315

316

317

318

319

320

321

322

323

324

325

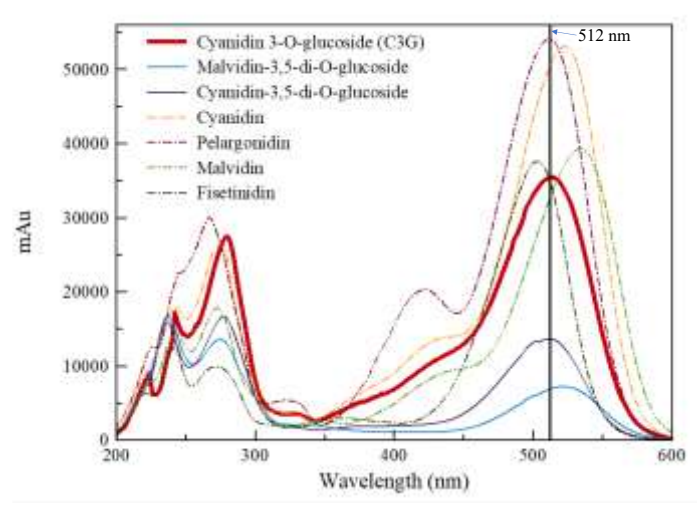


Figure 2. UV-Vis spectra of representative anthocyanins and anthocyanidins standards at the same molar concentration (1 μ M).

In this work, MRRFs of anthocyanins were determined by using a group of commercially available standards (Table S1). The molar response factors were computed based on the integrated absorbance of the chromatographic peak of each compound. The impact of hydroxylation, methylation, and glycosylation substitution on molar response factors was examined based on the known standards and then was derived into substitution-specific rules, which were extended to predict the MRRFs of compounds in the anthocyanin family (MRRFp). The discussion mainly focused on the MRRFs of anthocyanidins/anthocyanins at their respective λ_{max} . Another set of MRRF values was also computed using C3G as the master reference standard at 512 nm for all anthocyanins (MRRFc3G_512), which considered the λ_{max} shift in the calculation. The MRRFc3G_512 is more convenient to use in the applications of anthocyanin quantitation in food materials.

Table 1. Anthocyanidins and 3-O-, 3,5-O-glycosides with MRRF

	Mol. λ_{max} Substituents*								MRRF (λ_{max})		MRRF
Compound	Weight	(nm)	R_3	R_5	R_8	$R_{3'}$	$R_{4'}$	$R_{5'}$	Су	C3G	(C3G_512)
				A	Anthoc	yanidins					
Cyanidin (Cy)	287.2	523	ОН	ОН	Н	ОН	ОН	Н	1.00	1.37	
Apigeninidin (Ag)	255.3	471	Н	ОН	Н	Н	OH	Н	0.66	0.90	
Delphinidin (Dp)	303.2	531	OH	OH	Н	OH	ОН	ОН	1.13	1.55	
Diosmetinidin (Dm)	285.3	485	Н	OH	Н	OH	OMe	Н	0.74	1.02	
Fisetinidin (Fn)	271.3	503	OH	Н	Н	ОН	ОН	Н	0.71	0.97	
Gossypetinidin (Gp)	303.2	500	ОН	ОН	ОН	ОН	ОН	Н	0.50	0.69	
Luteolinidin (Ln)	271.3	486	Н	OH	Н	OH	ОН	Н	0.89	1.22	
Pelargonidin (Pg)	271.3	512	OH	OH	Н	Н	ОН	Н	1.02	1.39	
Peonidin (Pn)	301.3	525	OH	OH	Н	OMe	ОН	Н	0.88	1.21	
Petunidin (Pt)	317.3	531	ОН	ОН	Н	ОН	ОН	OMe	1.03	1.42	
Robinetinidin (Rn)	287.2	507	ОН	Н	Н	ОН	ОН	ОН	0.79	1.08	
Malvidin (Mv)	331.3	534	ОН	ОН	Н	OMe	ОН	OMe	0.77	1.06	
, ,					Antho	cyanins					
Cyanidin-3-O-	449.4	513	OGlu	ОН	Н	ОН	ОН	Н	0.73	1.00	1.00
glucoside (C3G)											
Cyanidin-3-O-	419.4	513	OAra	ОН	Н	OH	OH	Н	0.61	0.84	0.84
arabinoside	505.5	512	OD.	OH	**	OH	OH		0.61	0.04	0.04
Cyanidin-3- <i>O</i> -rutinoside	595.5	513	ORut	ОН	Н	ОН	ОН	Н	0.61	0.84	0.84
Cyanidin-3- <i>O</i> -	581.5	516	OSam	ОН	Н	ОН	ОН	Н	0.68	0.94	0.94
sambubioside	301.3	310	OSam	OH	11	OH	OH	11	0.00	0.74	0.74
Cyanidin-3- <i>O</i> -	743.6	511	OSam	OGlu	Н	ОН	ОН	Н	0.24	0.33	0.33
sambubioside -5- <i>O</i> -											
glucoside											
Cyanidin-3,5-di- <i>O</i> -	611.5	511	OGlu	OGlu	Н	OH	OH	Н	0.26	0.36	0.36
glucoside (C35G)	465.4	70 0	0.01	0.11	**	0.11	011	0.11	0.60	0.02	0.00
Delphinidin-3-O-	465.4	520	OGlu	ОН	Н	ОН	ОН	ОН	0.68	0.93	0.89
glucoside (D3G) Delphinidin-3- <i>O</i> -	611.5	524	ORut	ОН	Н	ОН	ОН	ОН	0.62	0.85	0.82
rutinoside	011.3	324	OKui	ОП	П	ОП	ОП	OH	0.02	0.83	0.82
Delphinidin-3- <i>O</i> -	597.5	524	OSam	ОН	Н	ОН	ОН	ОН	0.69	0.94	0.90
sambubioside	0,710	<i>-</i>	3 2	911		911	011	011	0.05	0.5.	0.50
Delphinidin-3-O-	759.6	522	OSam	OGlu	Н	ОН	ОН	ОН	0.29	0.40	0.38
sambubioside-5-O-											
glucoside											
Delphinidin-3,5-di-	627.5	520	OGlu	OGlu	Н	OH	OH	ОН	0.28	0.39	0.37
O-glucoside (D35G)	402.4	524	00.1	OH		0)/(OH	014	0.55	0.75	0.72
Malvidin-3- <i>O</i> -galactoside (M3Gal)	493.4	524	OGal	ОН	Н	OMe	ОН	OMe	0.55	0.75	0.72
Malvidin-3- <i>O</i> -	493.4	525	OGlu	ОН	Н	OMe	ОН	OMe	0.52	0.71	0.68
glucoside (M3G)	1/J:T	323	Oolu	011	11	OIVIC	O 11	OIVIC	0.52	0.71	0.00
Malvidin-3,5-di- <i>O</i> -	655.6	520	OGlu	OGlu	Н	OMe	ОН	OMe	0.10	0.14	0.13
glucoside (M35G)	-										
•											

Pelargonidin-3- <i>O</i> -glucoside (P3G)	433.4	502	OGlu	ОН	Н	Н	ОН	Н	0.61	0.83	0.78
Pelargonidin-3,5-di-	595.5	502	OGlu	OGlu	Н	Н	ОН	Н	0.36	0.50	0.47
O-glucoside (P35G)	462.4	515	0.01	OH	11	OM.	OH	11	0.74	1.02	1.02
Peonidin-3- <i>O</i> -glucoside (Pn3G)	463.4	515	OGlu	ОН	Н	OMe	ОН	Н	0.74	1.02	1.02
Peonidin-3,5-di-O-	625.6	512	OGlu	OGlu	Н	OMe	ОН	Н	0.29	0.40	0.40
glucoside (Pn35G)	450.4	7 00	0.01	0.11		0.11	0.11	03.6	0.55	0.76	0.50
Petunidin-3- <i>O</i> -	479.4	522	OGlu	ОН	Н	ОН	ОН	OMe	0.55	0.76	0.73
glucoside (Pt3G)											

^{*}Abbreviations: Ara, arabinoside; Me, methyl; Gal, galactoside; Glc, glucoside; Rut, rutinoside; Sam, sambubioside.

3.3.1. Hydroxyl substitution effect on MRRFs at λ_{max}

342

343

344

345

346

347

348

349

350

351

352

353

354

355

356

357

358

The MRRF values at λ_{max} relative to Cy are listed in Table 1. The -OH substitutions on 3' and 5' positions of the B-ring barely affected MRRF values, whereas variations of -OH on A- and Crings resulted in significant MRRF changes. When comparing the six pairs of Cy and Dp or Cybased anthocyanins and their Dp counterparts (e.g., MRRF_{Del}/MRRF_{Cy} and MRRF_{D3G}/MRRF_{C3G}) in Table 1, their ratios are 1.06 ± 0.09 , which suggests the 5' position -OH substitution on Dp aglycone does not have a significant effect on the molar absorptivity. The observation was also supported by comparing fisetinidin (Fn) and robinetinidin (Rn) with their MRRF value ratio at 1.10 (i.e., MRRF_{Rob}/MRRF_{Fis} = 0.79/0.71). Two pairs of anthocyanidins (i.e., Cy and Pg; Ap and Ln) and two pairs of anthocyanins (i.e., C3G and pelargonidin-3-O-glucoside (P3G); C35G and pelargonidin-3,5-di-O-glucoside (P35G)) only vary their structures at the 3' position by one -OH substitution and the average of their MRRF ratios is 1.1 ± 0.2 . Although the MRRF ratios in the four pairs show some discrepancy, the main reference standards of Cy and Pg consistently agree on MRRF values. Therefore, it is concluded that the -OH substitutions on the B-ring would not cause significant changes in molar absorptivity at their λ_{max} . Our data also show that the addition of -OH on B-ring (Pg \rightarrow Cy \rightarrow Dp, and their respective anthocyanins) is associated with a 7-15 nm bathochromic shift (red shift) of the λ_{max} . This shift could contribute to an error in quantitation

when only one wavelength (e.g., 512 nm) was used to monitor all anthocyanins, which is discussed in more detail in later sections.

The hydroxyl group on the A- and C-rings primarily substitutes at the 3, 5, 7, and 8 positions, and evidently, the lack of -OH at the 3 and 5 positions would alter the molar absorptivity and λ_{max} significantly. Losing -OH at the 5 position decreases MRRF values at λ_{max} about 30% when comparing between MRRF_{Cy} and MRRF_{Fn} and between MRRF_{Dp} and MRRF_{Rn} and shifts to shorter wavelengths (i.e., hypsochromic shift) by about 20 nm. The loss of -OH at the 3-position reduced the MRRF values by 11-35% when comparing between MRRF_{Cy} and MRRF_{Ln} and between MRRF_{pg} and MRRF_{Ag} and produced the hypsochromic shift by about 40 nm. Gossypetinidin has an additional -OH at the 8-position compared with Cy, which caused a 50% decrease in MRRF value and a hypsochromic shift by 23 nm. Overall, the hydroxylation substitutions on A- and C-rings lead to significant changes in anthocyanidins' MRRF values at their respective λ_{max} .

3.3.2. Methyl substitution effect on MRRFs at λ_{max}

Methylation on aglycones mainly derives from the -OH on the B-ring to form the methoxy groups. To study the methyl substitution effect on MRRFs, 8 pairs of MRRF values for compounds differing by one methyl group at 3', 4', or 5' position were compared (i.e., MRRF_{Pn}/MRRF_{Cy}, MRRF_{Dm}/MRRF_{Ln}, MRRF_{Pt}/MRRF_{Dp}, MRRF_{Mv}/MRRF_{Pt}, MRRF_{M3G}/MRRF_{Pt3G}, MRRF_{Pt3G}/MRRF_{D3G}, MRRF_{Pn3G}/MRRF_{C3G}, and MRRF_{Pn35G}/MRRF_{C35G}). The results showed a slight decrease in MRRF ratios (0.9 \pm 0.1) with an additional methyl group on the B-ring regardless of the position, and methylation on the B-ring did not shift λ_{max} ($\Delta\lambda_{max}$ <5 nm).

3.3.3. Glycoside substitution effect on MRRFs at λ_{max}

In nature, most anthocyanidins are present in glycosylated forms (i.e., their respective anthocyanins) except for a few 3-deoxyanthocyanidins such as Ag, diosmetinidin (Dm), and Ln found in mosses, ferns, and some flowering plants (Xiong, Zhang, Warner & Fang, 2019). For anthocyanins, glycosylation at the 3-position is most prevalent and additional sugar moieties can be attached to 5 or 7 positions to form diglycosidic anthocyanins (Saha, Singh, Paul, Sarkar, Khan & Banerjee, 2020). No 7-O-glycosylated anthocyanin standards were available, so this study focused on the 3-O-, and 5-O-glycoside substitution effect on MRRFs. In our previous reports, glycosylation for flavones, flavanones, and isoflavones was found to have little effect on the MRRF values at the λ_{max} (Lin & Harnly, 2012) (Zhang, M., Sun & Chen, 2015), but significant changes on MRRFs were observed for anthocyanins due to the glycosylation from the current study.

Twelve 3-O-glycosylated anthocyanin standards were acquired, including those derived from all six major anthocyanidins (i.e., 4 for Cy, 3 for Dp, 2 for Mv, and 1 for Pg, Pn, and Pt, Table 1). The mono- (i.e., galactoside, glucoside, or arabinoside) and bi- (i.e., rutinoside or sambubioside) glycoside substitutions at the 3-position notably reduced the molar absorptivity compared with their respective anthocyanidins with no exception, and the MRRF values at the λ_{max} decreased by $35\% \pm 8\%$. The results also indicated that the additional sugar moieties at the same substitution position, such as the rhamonsyl moiety in rutinoside and xylosyl moiety in sambubioside, did not affect the molar absorptivity or λ_{max} , which agreed with the observation of equal MRRF values between flavonol-glucosides and flavonol-rutinosides (Lin, Harnly, Zhang, Fan & Chen, 2012). Another seven 3,5-di-O-glycosylated anthocyanin standards were analyzed, and the results suggested that the additional glycosylation at the 5-position further decreased the MRRF values at the λ_{max} by another $60\% \pm 7\%$, leading to an average MRRF ratio of 3,5-di-O-glycosylated

anthocyanins to their respective aglycones at $26\% \pm 7\%$. While the 3-position glycoside substitution shifted the λ_{max} about 10 nm to blue compared to their respective anthocyanidins, the additional 5-position glycosylation had little effect on λ_{max} . Diglycosylated anthocyanins are very common in food and even present as the major anthocyanins in food like sweet cherry (94%), black current (76%), black raspberry (64%), red raspberry (52%), eggplant (83%), and small red beans (61%) (Wu, Beecher, Holden, Haytowitz, Gebhardt & Prior, 2006). To the best of our knowledge, the difference in molar absorptivity between mono- and di-glycosylated anthocyanins has never been reported previously, and its impact on anthocyanin quantitation is significant. For example, the anthocyanins in food extract were often quantified by one or several selected reference standards such as their respective anthocyanidins (i.e., Cy, Dp, and Mv) or monoglycosylated anthocyanins (i.e., C3G and M3G), and in both cases, the di-glycosylated anthocyanins were underestimated by 73% if quantified by anthocyanidins and by 35% if quantified by its respective mono-glycosylated anthocyanin at the λ_{max} . In some foods such as red cabbage and red radish, tri-glycosylated anthocyanins were also identified (Jing, Zhao, Ruan, Xie, Dong & (Lucy) Yu, 2012), which often had one sugar moiety substituted at the 3-position and two sugar moieties substituted at the 5-position. Since the bi-glycosides such as rutinoside and sambubioside did not affect the molar absorptivity or λ_{max} compared to the respective mono sugar moieties, the same MRRF values and λ_{max} of these tri-glycosylated anthocyanins were assigned based on their di-glycosylated anthocyanin counterparts.

3.3.4. Acylation effect on MRRFs at λ_{max}

404

405

406

407

408

409

410

411

412

413

414

415

416

417

418

419

420

421

422

423

424

425

426

Another group of anthocyanins has acylated sugar moieties on the aglycones, and they account for about 23% of total daily anthocyanin intake in the US based on the food intake data from the National Health and Nutrition Examination Survey (NHANES 2001-2002) (Wu, Beecher, Holden,

Haytowitz, Gebhardt & Prior, 2006). The acylated anthocyanins are commonly formed by the hydroxycinnamic acid (HCA) derivatives such as p-coumaric, caffeic, ferulic, and sinapic acids esterified to sugar moieties, and they are often considered more stable due to intramolecular copigmentation through blocking hydration of the flavylium cation (Houghton, Appelhagen & Martin, 2021). The co-pigmentation affects the UV-Vis absorbance in two ways: hyperchromism and bathochromism. In the food matrix, the hyperchromic shift is promoted by the favorable π stack interaction between aglycone and HCA, which drives the equilibrium toward the formation of more stable acylated anthocyanin flavylium cations from the neutral base (equilibrium constant K_{al}) and lowers the rate constant of water addition to the flavylium ion or hydration (equilibrium constant K_h (Moloney, Robbins, Collins, Kondo, Yoshida & Dangles, 2018). Due to the lack of reference standards, quantitative studies of the intramolecular hyperchromic effects between the chromophores of flavylium ions and HCA are rare, but the intermolecular co-pigmentation effects between anthocyanins and HCA have been extensively investigated (Lambert, Asenstorfer, Williamson, Iland & Jones, 2011, Sun, Cao, Bai, Liao & Hu, 2010). Despite the influences of anthocyanins and HCA types, the co-pigmentation reaction was dependent on pH, where the maximum UV-Vis absorbance enhancement was observed around pH 4, and no enhancement was found at low pH (<2) (Sun, Cao, Bai, Liao & Hu, 2010) In our study, the plant extract and reference standard samples were in the water/MeOH solution containing 10% FA (pH \approx 1.7) in which the acylated anthocyanin primarily exists in the flavylium form (i.e., K_{al} and K_h ranged 3.8-4.5 and 2.7-4.4, respectively) (Moloney, Robbins, Collins, Kondo, Yoshida & Dangles, 2018). Under this pH condition, the presence of the HCA group is not expected to significantly increase the flavylium form in the solution, therefore its enhancement on UV-Vis absorbance at λ_{max} is minimal, and the

427

428

429

430

431

432

433

434

435

436

437

438

439

440

441

442

443

444

445

446

447

MRRF values at the λ_{max} are considered unaffected by acylation under our experimental conditions.

449

450

451

452

453

454

455

456

457

458

459

460

461

462

463

464

465

466

467

468

469

470

471

The bathochromic shift of the visible band of acylated anthocyanin is a result of the reduced excitation energy gap between the highest occupied molecular orbital and the lowest unoccupied molecular orbital due to the partial mixing of the π orbitals of the two interacting conjugated systems (i.e., aglycone and HCA) (Silva, Freitas, Maçanita & Quina, 2016). The UV-Vis spectra of acylated anthocyanins from the red cabbage extract are shown in Figure S3. The bathochromic shift due to the HCA moieties appears to be additive and HCA-type dependent. For example, the mono sinapoyl (sin) and di-sinapoyl anthocyanins have visible λ_{max} around 524 nm and 535 nm, respectively, indicating about 12-nm redshift per sin group added with respect to their nonacylated anthocyanins. Overall, the caffeoyl (caf), feruloyl (fer), coumaroyl (cou), and sin groups caused a bathochromic shift (~10 nm) to anthocyanin spectra, and the results agree with the previously published values (Steingass et al., 2023). The acylation with non-HCA, such as acetyl and malonyl groups, was expected to have a minimal impact on wavelength shift due to the lack of a conjugated system to interact with aglycone (Hong, Netzel & O'Hare, 2020, Zhu et al., 2012). Steingass et al. also reported p-hydroxybenzoyl (phb) group also had a weak impact on the bathochromic shift (~5 nm), and the tri- and tetra-HCA acylated anthocyanins would not significantly change the visible λ_{max} (i.e., <5 nm) compared to the di-HCA acylated anthocyanin counterparts (Steingass et al., 2023). Since there are only two lobes for the π orbitals of aglycones, it is reasonable to expect each aglycone to only interact with two HCA chromophores at maximum. Based on the literature and results from our study, the rules below apply to the acylated anthocyanins for the convenience of MRRF calculation: a) acetyl and malonyl groups have no effects on wavelength shift; b) each phb results in 5 nm bathochromic shift and each fer/cou/sin/caf results in 10 nm bathochromic shift; c) the visible λ_{max} of acylated anthocyanin with more than two HCA group is approximately the same as its di-HCA counterparts.

3.3.5. MRRFs relative to C3G at 512 nm (MRRF_{C3G 512})

472

473

474

475

476

477

478

479

480

481

482

483

484

485

486

487

488

489

490

491

492

493

494

MRRF values at λ_{max} are critical to understanding the effects of function groups on the molar absorptivity; however, they are inconvenient to use directly in the quantitative studies due to the wavelength variations in λ_{max} for different anthocyanins. It is a cumbersome process for each anthocyanin to identify the λ_{max} from each UV-Vis spectrum, extract the chromatogram at that specific λ_{max} , integrate the peak area, and then determine the concentration based on the external calibration. The DAD is needed for this process. It will greatly simplify the process if only one specific wavelength is used when quantifying the anthocyanin peaks from the chromatograms instead of using various λ_{max} for different anthocyanins, which also enables the routine analysis of anthocyanins with less expensive UV-Vis detectors such as fixed or variable wavelength detectors. To apply the MRRF strategy at one standard wavelength, we propose another set of MRRF values at 512 nm relative to a master reference standard (C3G) or MRRF_{C3G} 512. The difference in molar absorptivity at λ_{max} and 512 nm can introduce quantitative error if not corrected. For example, the absorbance for M35G decreases at 512 nm compared to its absorbance at its λ_{max} (Figure 2). Therefore, MRRF_{C3G} 512 values were computed by incorporating substitution and wavelength variation effects, as discussed below. The first step is calculating the MRRF of anthocyanidins/anthocyanins relative to C3G at their respective λ_{max} (MRRF_{C3G} λ_{max}). A conversion factor $\alpha_{CV\to C3G}$ is needed and defined as the absorbance ratio between Cy and C3G at their λ_{max} at the same molar concentration. The $\alpha_{Cv\to C3G}$ was computed to be 1.37 based on the experimental data. Since the MRRF values of the known anthocyanidins/anthocyanins relative to Cy (MRRF_{Cy \lambdamax}) have been measured in Table 1, these

values multiplied by $\alpha_{C\nu\to C3G}$ give their MRRF_{C3G_\lambdamax} respectively. The next step is to correct their molar absorptivity differences between the λ_{max} and 512 nm. The six major classes of anthocyanins can be grouped into 3 categories based on their λ_{max} . Cy- and Pn-based anthocyanins have the λ_{max} at about 512 nm, so no correction applies. The λ_{max} for Dp-, Mv-, and Pt-based anthocyanins redshift about 10 nm to 522 nm, whereas those for Pg-based anthocyanins blue shift 10 nm to 502 nm (Figure S4A). To study the shift effects, the UV-Vis spectra in the range of 480-550 nm of the anthocyanins in Table 1 were fit to an unconditioned Gaussian curve, and the absorbance decrease caused by the 10 nm shift was calculated based on their Gaussian functions, respectively. For example, the Gaussian fit curve of the M3G UV-Vis spectrum is shown in Figure S4C, and UV-Vis absorbance at 512 nm is about 4% lower than the absorbance at its λ_{max} . Figure S4D shows the results for P3G, which indicates a 7% decrease in absorbance at 512 nm compared with that at its λ_{max} . The average decrease of absorbance for Dp-, Mv-, and Pt-based anthocyanins at 512 nm is $4\% \pm 1\%$, and the decrease of absorbance for Pg-based anthocyanins at 512 nm is 7% (standard deviation not calculated since only two Pg-anthocyanins are available). The factor to correct the absorbance difference between λ_{max} and 512 nm is defined as $\beta_{\lambda max \to 512}$ (i.e., 4% for Dp, Mv, and Pt-based anthocyanins and 7% for Pg-anthocyanins). The 3-deoxyanthocyanidins such as Ag, Dm, and Ln and their glycosides are rare in nature (Herrman, Brantsen, Ravisankar, Lee & Awika, 2020), and the lack of a hydroxyl group on the 3 position results in a strong blue shift (i.e., 30-40 nm) at λ_{max} compared to 512 nm (Figure S4B). For example, the $\beta_{\lambda \text{max} \to 512}$ for Ag, Dm, and Ln was determined as 40%, 40%, and 75%, respectively (Figure S4E and F). The $\beta_{\lambda max \to 512}$ for acylated anthocyanins were calculated similarly based on the UV-Vis spectra in Figure S3 and a list of $\beta_{\lambda max \to 512}$ used to predict MRRF_{C3G_512} for anthocyanins is provided in Table S2. Finally, the MRRF_{C3G_512} is calculated as: $MRRF_{C3G_512} = MRRF_{Cy} \times \alpha_{Cy \to C3G} \times (1 - 1)$

495

496

497

498

499

500

501

502

503

504

505

506

507

508

509

510

511

512

513

514

515

516

 $\beta_{\lambda \text{max} \to 512}$). With this equation, we can extend to predict the MRRF_{C3G_512} for anthocyanins without reference standards. For example, delphinidin 3-*O*-rutinoside 5-*O*-glucoside (C₃₃H₄₁O₂₁, CAS Registry No. 29837-24-9) has two sugar moieties at 3- and 5- positions on Dp, so its $MRRF_{Cy} = 1.13 \times (1 - 35\%) \times (1 - 60\%) \approx 0.29$, whereas 1.13 is $MRRF_{Cy}$ from Dp and (1 - 35%) and (1 - 60%) represent the MRRF decrease due to the glycosyl substitutions at 3 and 5 position, respectively. Then its $MRRF_{C3G_512}$ can be calculated as $MRRF_{Cy} \times \alpha_{Cy \to C3G} \times (1 - \beta_{\lambda \text{max} \to 512}) = 0.2938 \times 1.37 \times (1 - 5\%) \approx 0.38$.

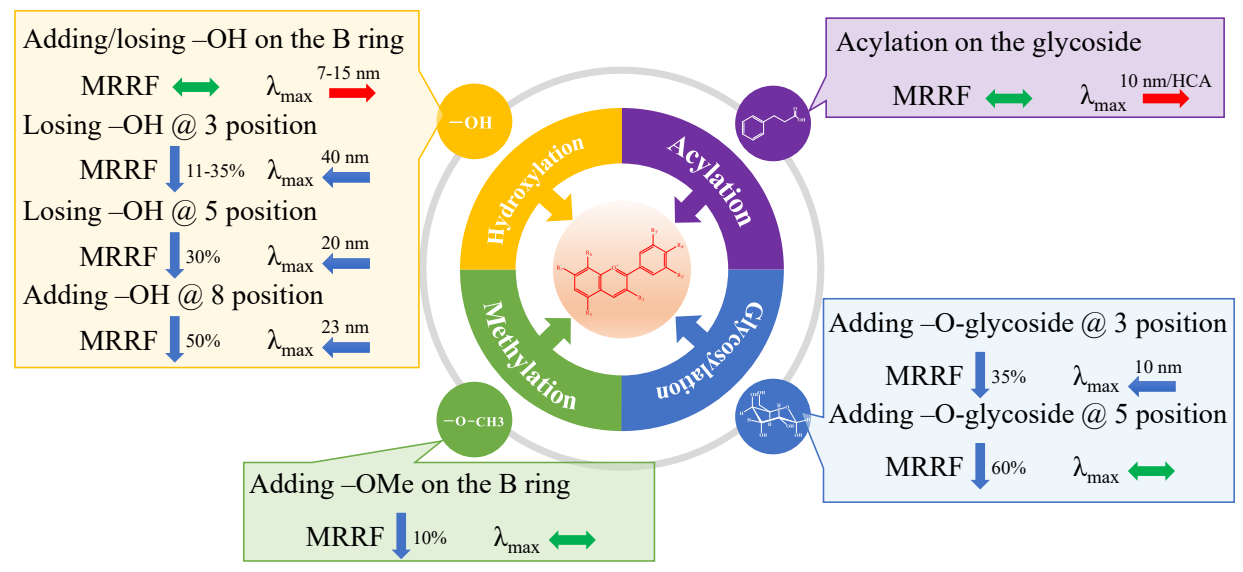


Figure 3. General rules for MRRF and λ_{max} shift due to the structural variations for anthocyanins.

3.3.6. Expansion of MRRFs to the anthocyanin family and recommended protocol

The influences of anthocyanin structural variation on MRRF and λ_{max} are summarized in Figure 3. These rules laid the foundation to compute MRRF values for the compounds in the anthocyanin family. $MRRF_{C3G_512}$ for 617 anthocyanins/anthocyanidins were predicted based on the rules and strategies developed in this study, and the information is incorporated into an online anthocyanin library available at https://BotanicalDC.online/anthocyanin/. The list of anthocyanins was gathered from the literature, public database, and our research, and will be expanded as new

anthocyanins are reported. The six major types of anthocyanins account for 91% of total anthocyanins in the library, and their respective glycosylation types are listed in Figure S5. In addition to MRRFs, this web-based library consists of chemical identification information for anthocyanins, such as exact mass, synonym, formula, CAS number, structure, InChIKey, InChICode, simplified molecular-input line-entry system (SMILES), and links to FoodB, PubChem, and Knaspsack databases. These chemical identifiers are critical to avoid the ambiguity of scientific communication in food chemistry because the inconsistent use of nomenclature in the description of flavonoids has long been an issue in scientific reports (Balentine et al., 2015). The search menu allows users to perform a name search, a formula search, a CAS number search, or combined and thus obtain an output table for matched anthocyanin records with formula, CAS number, MRRF, and links to detailed chemical information for each anthocyanin. All the information is freely available.

To employ the $MRRF_{C3G_512}$ strategy in the anthocyanin research, the protocol below is recommended. First, plant extract and C3G calibration samples are detected by HPLC/UV at 512 nm. Secondly, the calibration curve for C3G is constructed based on the peak areas. Third, the concentrations of target anthocyanins can be determined as

$$C_{target} = \frac{C_{C3G} \times MW_{target}}{MRRF_{C3G_512}} \times MW_{C3G}$$

where C_{C3G} is the concentration of the compound as calculated from the C3G calibration curve, MW_{C3G} is the molecular weight of C3G, MW_{target} is the molecular weight of the target anthocyanin, and $MRRF_{C3G_512}$ for the target anthocyanin can be found in our online library. In previous research, the anthocyanin content in food was often expressed as milligrams of selected anthocyanin/anthocyanidin equivalents per 100-gram dry matter; however, various reference anthocyanin/anthocyanidin were used, such as C3G (Grace, Xiong, Esposito, Ehlenfeldt & Lila,

2019), cyanidin (Steingass et al., 2023), and M3G (Lee, Rennaker & Wrolstad, 2008), which caused a great challenge to compare results among different studies. The C_{target} calculated in our strategy should be considered as a close estimate of the concentration of individual anthocyanin instead of the equivalence to the C3G because of the incorporation of MRRF and molecular weight conversion. The total anthocyanins for the plant materials are calculated by summing up individual anthocyanin content and should not be expressed as C3G equivalent. The implementation of molecular weight correction was considered more accurate for anthocyanin quantification (Wu, Beecher, Holden, Haytowitz, Gebhardt & Prior, 2006). The MRRF strategy further improved the quantification accuracy and eliminated the ambiguity of anthocyanin content expression. In addition, the MRRFs of anthocyanins introduce a pathway to convert anthocyanin contents in different literature to a uniform expression for comparison, food survey, protocol standardization, etc.

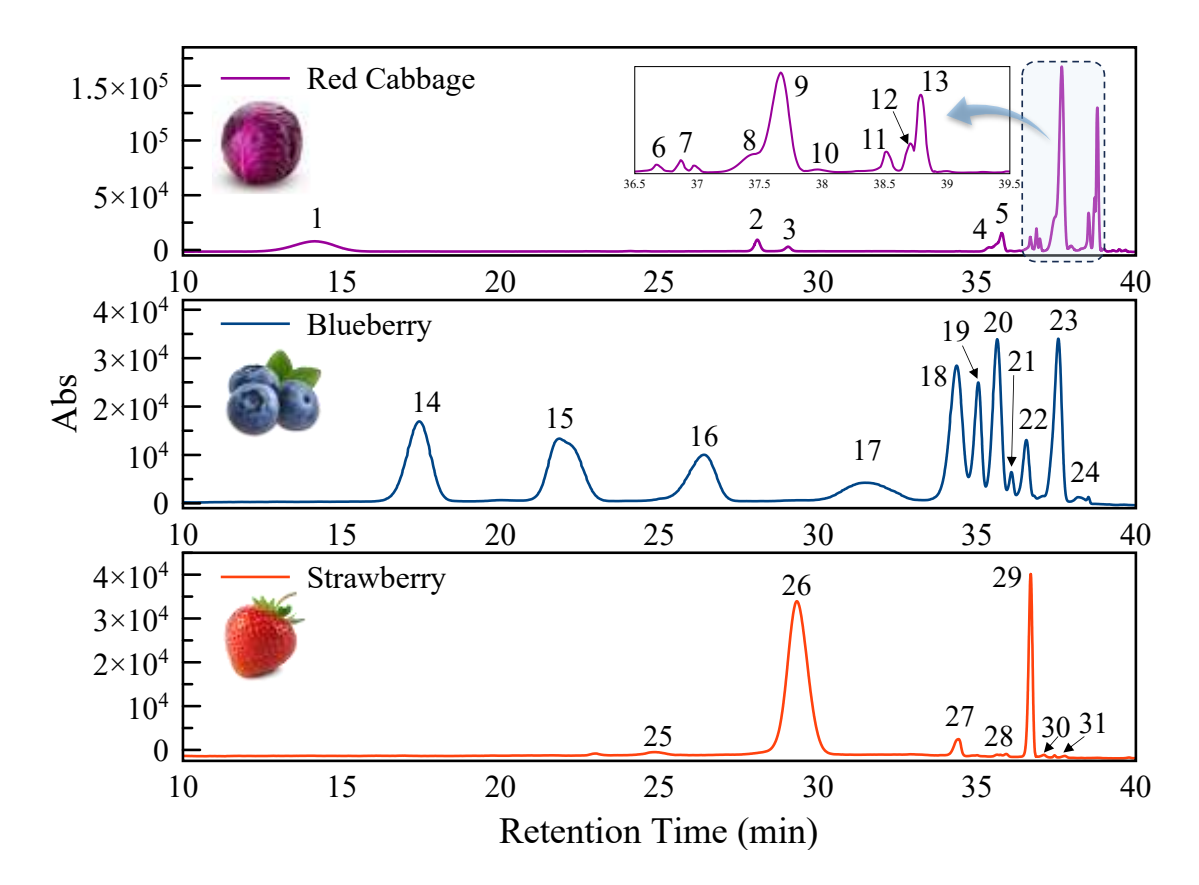


Figure 4. Chromatograms of red cabbage, blueberry, and strawberry at 512 nm. Refer to Table 2 and Table S3 for the identification of each peak labeled.

3.4. Quantitative analysis of anthocyanins in foods

Anthocyanins were quantified in blueberry, strawberry, and red cabbage by comparison to the master standard (i.e., C3G) calibration curve with and without MRRF correction. Figure 4 shows chromatograms for the three foods, and Tables 2 and S3 list the identified anthocyanins and computed concentrations. MRRF strategy has especially significant impacts on the quantitation of complex anthocyanins with high molecular weights for which the concentrations were underestimated by the traditional quantitative approach. For example, the anthocyanins in red cabbages exist predominantly as acylated di- or tri-glycosides, which tend to have low $MRRF_{C3G_512}$ values due to the reduced molar absorptivity caused by the 3- and/or 5- position

glycoside and λ_{max} shift effect on molar absorptivity. With the MRRF correction, the concentration of cyanidin 3-sophoroside 5-glucoside in red cabbage was about 2.8 times higher than that without correction (307 \pm 3 mg/100 g vs 109 \pm 1 mg/100 g, Table 2 Peak ID 1).

577

578

579

580

581

582

583

584

585

586

587

588

589

590

591

592

593

594

Overall, the total anthocyanin concentration in red cabbages with MRRF correction was over 200% higher than without MRRF correction. It is important to note that the MRRF strategy is also effective in quantifying anthocyanins with different aglycones by one master standard. For example, the M3Gal in the blueberry extract (Peak ID 18 in Figure 4 and Table S3) was determined to be 68 ± 6 mg/100 g and 104 ± 9 mg/100 g when using C3G calibration for the quantitation with and without MRRF correction, respectively. The same peak was quantified by using the M3Gal external calibration curve, and the concentration was used as the reference value ($106 \pm 10 \text{ mg}/100$ g). The quantitative accuracy for this peak was calculated as relative errors, showing 36% and 2%, respectively, before and after applying the MRRF correction based on the C3G calibration curve, which indicates a significant improvement in M3Gal quantitation accuracy. The total anthocyanins based on MRRF values for blueberry and strawberry extracts were consistently higher, 23% and 19%, respectively, than those calculated by C3G external calibration without MRRF correction. Therefore, the MRRF strategy has shown great promise in addressing the quantitative errors caused by the molar absorptivity variation and providing more accurate anthocyanin quantification results in food materials.

Table 2. Quantification of individual and total anthocyanin contents in red cabbage.

Plant Name	Peak ID	RT (min)	Anthocyanins	λ_{max} (nm)	Accurate Mass [M] ⁺	Molecular Formula	MRRF _p (C3G_512nm)	$\begin{array}{c} C_{\text{w/o MRRF}} \\ (\text{mg/100 g})^{\text{a}} \end{array}$	C _{w. MRRFC3G_512} (mg/100 g) ^a	Difference (%) ^b
Red cabbage	1	14.15	Cyanidin 3-sophoroside 5-glucoside	512	773.2135	$C_{33}H_{41}O_{21}^{+}$	0.36	109 ± 1	307 ± 3	182
	2	28.07	Cyanidin 3-(sinapoyl)- diglucoside-5-glucoside isomer	524	979.2831	C ₄₄ H ₅₁ O ₂₅ ⁺	0.34	20.3 ± 0.5	60 ± 1	195
	3	29.04	Cyanidin 3-(caffeoyl)(p-coumaroyl)-diglucoside-5-glucoside	530	1081.3031	C48H57O28 ⁺	0.30	8.1 ± 0.5	27 ± 2	232
	4	35.39	Cyanidin 3-(sinapoyl)- triglucoside-5-glucoside	520	1141.3242	$C_{50}H_{61}O_{30}^{+}$	0.34	6.0 ± 0.2	17.6 ± 0.6	192
	5	35.8	Cyanidin 3- (feruloyl)(feruloyl)- triglucoside-5-glucoside	528	1287.3610	$C_{59}H_{67}O_{32}^{+}$	0.30	46.7 ± 0.3	154 ± 1	230
	6	36.68	Cyanidin 3- (feruloyl)(sinapoyl)- triglucoside-5-glucoside	530	1317.3716	$C_{60}H_{69}O_{33}^{+}$	0.30	17.5 ± 0.4	58± 1	232
	7	36.87	Cyanidin 3-(signapoyl) (sinapoyl)-triglucoside-5-glucoside	534	1347.3821	$C_{61}H_{71}O_{34}^{+}$	0.30	14.1 ± 0.2	46.6 ± 0.7	230
	8	37.47	Cyanidin 3-(p-coumaroyl)-diglucoside-5-glucoside	522	919.2503	$C_{42}H_{47}O_{23}^{+}$	0.34	5.2 ± 0.1	15.2 ± 0.3	192
	9a	37.66	Cyanidin 3-(sinapoyl)-diglucoside-5-glucoside isomer	522	979.2831	$C_{44}H_{51}O_{25}^{+}$	0.34	238 ± 2	700 ± 6	194
	9b		Cyanidin 3-(feruloyl)-diglucoside-5-glucoside		949.2608	$C_{43}H_{49}O_{24}^{+}$	0.34	89.5 ± 0.7	262 ± 2	193

10	37.95	Cyanidin 3-(feruloyl)- triglucosides-5-glucoside	524	1111.3137	$C_{49}H_{59}O_{29}^{+}$	0.34	3 ± 1	10 ± 3	233
11	38.51	Cyanidin 3- (feruloyl)(feruloyl)-	534	1125.3082	$C_{53}H_{57}O_{27}^{+}$	0.30	33.2 ± 0.7	110 ± 2	232
12	38.71	diglucoside-5-glucoside Cyanidin 3-(feruloyl) (sinapoyl)-diglucoside-5- glucoside	534	1155.3187	$C_{54}H_{59}O_{28}^{+}$	0.30	42 ± 4	140 ± 12	233
13	38.78	Cyanidin 3- (sinapoyl)(sinapoyl)- diglucoside-5-glucoside	536	1185.3293	$C_{55}H_{61}O_{29}^{+}$	0.30	128 ± 3	420 ± 10	228
		Total					760 ± 10	2320 ± 32	205

^a Standard deviation (n = 5); ^b Comparison between $C_{w/o\ MRRF}$ and $C_{w.\ MRRFC3G_512}$ calculated as: $(C_{w/o\ MRRF} - C_{w.\ MRRFC3G_512})/C_{w/o\ MRRF}$.

4. Conclusion

596

597

598

599

600

601

602

603

604

605

606

607

608

609

610

611

612

613

614

615

617

In this work, the UV-Vis absorbance of anthocyanins was systematically examined, and the factors impacting the molar absorptivity were studied based on the anthocyanin reference standards. The derived general rules were extended to predict the MRRF values for the compounds in the anthocyanin family. An online library for 617 anthocyanins/anthocyanidins assigned with along with other chemical identifier information is free to https://BotanicalDC.online/anthocyanin/, and it can be a key resource for anthocyanin identification and quantitation. The database will be expanded with the rules developed as new anthocyanins are discovered. In addition, a simple yet comprehensive protocol based on the HPLC-UV-Vis and MRRF for quantifying anthocyanin with improved accuracy is proposed. The method requires monitoring only one single wavelength (i.e., 512 nm) and using only one master reference standard for calibration (i.e., C3G). This approach allows efficient and accurate quantitative analysis of anthocyanins in food materials without using individual reference standards and multiple calibration curves. Such a method could significantly benefit reporting anthocyanin values in food materials in the future, and it may also be used to update anthocyanin values in food materials from previous research literature where applicable. This work could provide a critical foundation for the development of new standard/reference methods for anthocyanin analysis in the food industry and government agencies and an important step to harmonize different analytical approaches for a better comparison of results and data from various sources.

Data availability Statement

Data will be made available on request.

CRediT authorship contribution statement

618 Methodology, W.D. and M.Z.; formal analysis, W.D., X.Y., N.Z., and M.Z.; data curation, W.D. 619 and M.Z.; conceptualization, P.C., J.S., J.H., and M.Z.; writing—original draft preparation, 620 W.D.; writing—review and editing, W.D., X.Y., N.Z., P.C., J.S., J.H., and M.Z.; supervision, 621 M.Z.; funding acquisition, P.C., J.H., and M.Z. All authors have read and agreed to the published 622 version of the manuscript. 623 **Declaration of competing interest** The authors declare that they have no known competing financial interests or personal 624 625 relationships that could have appeared to influence the work reported in this paper. 626 Acknowledgments 627 This work was supported by the Middle Tennessee State University (MTSU), the Agricultural 628 Research Service of the US Department of Agriculture, and an Interagency Agreement with the 629 Office of Dietary Supplements of the National Institute of Health. We acknowledge the NSF 630 MRI grant (Award Number: 2216092) to MTSU for the acquisition of a high-resolution mass 631 spectrometer. 632 Appendix A. Supplementary data 633 Supplementary data to this article can be found online at https://doi.org/10.1016/j.foodchem.xxx 634 References 635 Balentine, D. A., Dwyer, J. T., Erdman, J. W., Ferruzzi, M. G., Gaine, P. C., Harnly, J. M., &

Kwik-Uribe, C. L. (2015). Recommendations on reporting requirements for flavonoids in

- 637 research2. The American Journal of Clinical Nutrition, 101(6), 1113-1125,
- 638 doi:10.3945/ajcn.113.071274.
- 639 Cai, D., Li, X., Chen, J., Jiang, X., Ma, X., Sun, J., Tian, L., Vidyarthi, S. K., Xu, J., Pan, Z., &
- Bai, W. (2022). A comprehensive review on innovative and advanced stabilization approaches of
- anthocyanin by modifying structure and controlling environmental factors. Food Chemistry, 366,
- 642 130611, doi:10.1016/j.foodchem.2021.130611.
- 643 Castañeda-Ovando, A., Pacheco-Hernández, M. d. L., Páez-Hernández, M. E., Rodríguez, J. A.,
- & Galán-Vidal, C. A. (2009). Chemical studies of anthocyanins: A review. *Food Chemistry*,
- 645 113(4), 859-871, doi:10.1016/j.foodchem.2008.09.001.
- 646 Chandra Singh, M., Probst, Y., Price, W. E., & Kelso, C. (2022). Relative comparisons of
- extraction methods and solvent composition for Australian blueberry anthocyanins. *Journal of*
- 648 Food Composition and Analysis, 105, 104232, doi:10.1016/j.jfca.2021.104232.
- 649 Chandra, A., Rana, J., & Li, Y. (2001). Separation, Identification, Quantification, and Method
- Validation of Anthocyanins in Botanical Supplement Raw Materials by HPLC and HPLC–MS.
- 651 *Journal of Agricultural and Food Chemistry*, 49(8), 3515-3521, doi:10.1021/jf010389p.
- 652 Chen, W., Su, H., Xu, Y., Bao, T., & Zheng, X. (2016). Protective effect of wild raspberry
- 653 (Rubus hirsutus Thunb.) extract against acrylamide-induced oxidative damage is potentiated
- after simulated gastrointestinal digestion. Food Chemistry, 196, 943-952,
- doi:10.1016/j.foodchem.2015.10.024.

- 656 Gowd, V., Jia, Z., & Chen, W. (2017). Anthocyanins as promising molecules and dietary
- 657 bioactive components against diabetes A review of recent advances. Trends in Food Science &
- 658 *Technology*, 68, 1-13, doi:10.1016/j.tifs.2017.07.015.
- 659 Grace, M. H., Xiong, J., Esposito, D., Ehlenfeldt, M., & Lila, M. A. (2019). Simultaneous LC-
- MS quantification of anthocyanins and non-anthocyanin phenolics from blueberries with widely
- divergent profiles and biological activities. *Food Chemistry*, 277, 336-346,
- doi:10.1016/j.foodchem.2018.10.101.
- Han, F., Yang, P., Wang, H., Fernandes, I., Mateus, N., & Liu, Y. (2019). Digestion and
- absorption of red grape and wine anthocyanins through the gastrointestinal tract. *Trends in Food*
- *Science & Technology*, 83, 211-224, doi:10.1016/j.tifs.2018.11.025.
- He, J., & Giusti, M. M. (2010). Anthocyanins: Natural Colorants with Health-Promoting
- Properties. Annual Review of Food Science and Technology, 1(1), 163-187,
- doi:10.1146/annurev.food.080708.100754.
- Herrman, D. A., Brantsen, J. F., Ravisankar, S., Lee, K., & Awika, J. M. (2020). Stability of 3-
- deoxyanthocyanin pigment structure relative to anthocyanins from grains under microwave
- assisted extraction. *Food Chemistry*, 333, 127494, doi:10.1016/j.foodchem.2020.127494.
- Hong, H. T., Netzel, M. E., & O'Hare, T. J. (2020). Optimisation of extraction procedure and
- development of LC–DAD–MS methodology for anthocyanin analysis in anthocyanin-pigmented
- 674 corn kernels. *Food Chemistry*, 319, 126515, doi:10.1016/j.foodchem.2020.126515.

- Houghton, A., Appelhagen, I., & Martin, C. (2021). Natural Blues: Structure Meets Function in
- 676 Anthocyanins. *Plants*, 10(4), doi:10.3390/plants10040726.
- 677 Jing, P., Zhao, S., Ruan, S., Xie, Z., Dong, Y., & (Lucy) Yu, L. (2012). Anthocyanin and
- 678 glucosinolate occurrences in the roots of Chinese red radish (Raphanus sativus L.), and their
- 679 stability to heat and pH. *Food Chemistry*, 133(4), 1569-1576,
- 680 doi:10.1016/j.foodchem.2012.02.051.
- Jokioja, J., Linderborg, K. M., Kortesniemi, M., Nuora, A., Heinonen, J., Sainio, T., Viitanen,
- 682 M., Kallio, H., & Yang, B. (2020). Anthocyanin-rich extract from purple potatoes decreases
- postprandial glycemic response and affects inflammation markers in healthy men. *Food*
- 684 *Chemistry*, 310, 125797, doi:10.1016/j.foodchem.2019.125797.
- Keunchkarian, S., Reta, M., Romero, L., & Castells, C. (2006). Effect of sample solvent on the
- chromatographic peak shape of analytes eluted under reversed-phase liquid chromatogaphic
- 687 conditions. *Journal of Chromatography A*, 1119(1), 20-28, doi:10.1016/j.chroma.2006.02.006.
- Khoo, H. E., Azlan, A., Tang, S. T., & Lim, S. M. (2017). Anthocyanidins and anthocyanins:
- colored pigments as food, pharmaceutical ingredients, and the potential health benefits. Food &
- 690 *nutrition research*, 61(1), 1361779, doi:10.1080/16546628.2017.1361779.
- Lambert, S. G., Asenstorfer, R. E., Williamson, N. M., Iland, P. G., & Jones, G. P. (2011).
- 692 Copigmentation between malvidin-3-glucoside and some wine constituents and its importance to
- 693 colour expression in red wine. *Food Chemistry*, 125(1), 106-115,
- 694 doi:10.1016/j.foodchem.2010.08.045.

- Lee, J., Rennaker, C., & Wrolstad, R. E. (2008). Correlation of two anthocyanin quantification
- 696 methods: HPLC and spectrophotometric methods. Food Chemistry, 110(3), 782-786,
- 697 doi:10.1016/j.foodchem.2008.03.010.
- Lee, J., Durst, R. W., Wrolstad, R. E., & Collaborators: (2005). Determination of Total
- Monomeric Anthocyanin Pigment Content of Fruit Juices, Beverages, Natural Colorants, and
- 700 Wines by the pH Differential Method: Collaborative Study. *Journal of AOAC International*,
- 701 88(5), 1269-1278, doi:10.1093/jaoac/88.5.1269.
- 702 Lin, L., & Harnly, J. M. (2012). Quantitation of Flavanols, Proanthocyanidins, Isoflavones,
- 703 Flavanones, Dihydrochalcones, Stilbenes, Benzoic Acid Derivatives Using Ultraviolet
- Absorbance after Identification by Liquid Chromatography–Mass Spectrometry. *Journal of*
- 705 Agricultural and Food Chemistry, 60(23), 5832-5840, doi:10.1021/jf3006905.
- Lin, L., Harnly, J., Zhang, R., Fan, X., & Chen, H. (2012). Quantitation of the Hydroxycinnamic
- 707 Acid Derivatives and the Glycosides of Flavonols and Flavones by UV Absorbance after
- 708 Identification by LC-MS. Journal of Agricultural and Food Chemistry, 60(2), 544-553,
- 709 doi:10.1021/jf204612t.
- 710 Lin, L., Sun, J., Chen, P., & Harnly, J. (2011). UHPLC-PDA-ESI/HRMS/MSn Analysis of
- 711 Anthocyanins, Flavonol Glycosides, and Hydroxycinnamic Acid Derivatives in Red Mustard
- 712 Greens (Brassica juncea Coss Variety). *Journal of Agricultural and Food Chemistry*, 59(22),
- 713 12059-12072, doi:10.1021/jf202556p.

- Marko, D., Puppel, N., Tjaden, Z., Jakobs, S., & Pahlke, G. (2004). The substitution pattern of
- anthocyanidins affects different cellular signaling cascades regulating cell proliferation.
- 716 *Molecular Nutrition & Food Research*, 48(4), 318-325, doi:10.1002/mnfr.200400034.
- 717 Merken, H. M., Merken, C. D., & Beecher, G. R. (2001). Kinetics Method for the Quantitation of
- 718 Anthocyanidins, Flavonols, and Flavones in Foods. *Journal of Agricultural and Food Chemistry*,
- 719 49(6), 2727-2732, doi:10.1021/jf001266s.
- Moloney, M., Robbins, R. J., Collins, T. M., Kondo, T., Yoshida, K., & Dangles, O. (2018). Red
- 721 cabbage anthocyanins: The influence of d-glucose acylation by hydroxycinnamic acids on their
- structural transformations in acidic to mildly alkaline conditions and on the resulting color. *Dyes*
- 723 and Pigments, 158, 342-352, doi:10.1016/j.dyepig.2018.05.057.
- Saha, S., Singh, J., Paul, A., Sarkar, R., Khan, Z., & Banerjee, K. (2020). Anthocyanin Profiling
- 725 Using UV-Vis Spectroscopy and Liquid Chromatography Mass Spectrometry. *Journal of AOAC*
- 726 *International*, 103(1), 23-39, doi:10.5740/jaoacint.19-0201.
- 727 Silva, V. O., Freitas, A. A., Maçanita, A. L., & Quina, F. H. (2016). Chemistry and
- 728 photochemistry of natural plant pigments: the anthocyanins. *Journal of Physical Organic*
- 729 *Chemistry*, 29(11), 594-599, doi:10.1002/poc.3534.
- 730 Steingass, C. B., Burkhardt, J., Bäumer, V., Kumar, K., Mibus-Schoppe, H., Zinkernagel, J.,
- 731 Esquivel, P., Jiménez, V. M., & Schweiggert, R. (2023). Characterisation of acylated
- anthocyanins from red cabbage, purple sweet potato, and Tradescantia pallida leaves as natural
- 733 food colourants by HPLC-DAD-ESI(+)-QTOF-MS/MS and ESI(+)-MSn analysis. Food
- 734 *Chemistry*, 416, 135601, doi:10.1016/j.foodchem.2023.135601.

- Sun, J., Cao, X., Bai, w., Liao, X., & Hu, X. (2010). Comparative analyses of copigmentation of
- cyanidin 3-glucoside and cyanidin 3-sophoroside from red raspberry fruits. *Food Chemistry*,
- 737 120(4), 1131-1137, doi:10.1016/j.foodchem.2009.11.031.
- 738 Trikas, E. D., Papi, R. M., Kyriakidis, D. A., & Zachariadis, G. A. (2016). A Sensitive LC-MS
- 739 Method for Anthocyanins and Comparison of Byproducts and Equivalent Wine Content.
- 740 *Separations*, 3(2), doi:10.3390/separations3020018.
- Wang, H., Sun, S., Zhou, Z., Qiu, Z., & Cui, X. (2020). Rapid analysis of anthocyanin and its
- structural modifications in fresh tomato fruit. Food Chemistry, 333, 127439,
- 743 doi:10.1016/j.foodchem.2020.127439.
- 744 Wu, X., Beecher, G. R., Holden, J. M., Haytowitz, D. B., Gebhardt, S. E., & Prior, R. L. (2006).
- 745 Concentrations of Anthocyanins in Common Foods in the United States and Estimation of
- Normal Consumption. Journal of Agricultural and Food Chemistry, 54(11), 4069-4075,
- 747 doi:10.1021/jf0603001.
- 748 Wu, X., Gu, L., Prior, R. L., & McKay, S. (2004). Characterization of Anthocyanins and
- 749 Proanthocyanidins in Some Cultivars of Ribes, Aronia, and Sambucus and Their Antioxidant
- 750 Capacity. Journal of Agricultural and Food Chemistry, 52(26), 7846-7856,
- 751 doi:10.1021/jf0486850.
- Wu, X., Cao, G., & Prior, R. (2002). Absorption and Metabolism of Anthocyanins in Elderly
- Women after Consumption of Elderberry or Blueberry. *The Journal of nutrition*, 132, 1865-71,
- 754 doi:10.1093/jn/132.7.1865.

- 755 Xiong, Y., Zhang, P., Warner, R. D., & Fang, Z. (2019). 3-Deoxyanthocyanidin Colorant:
- 756 Nature, Health, Synthesis, and Food Applications. Comprehensive Reviews in Food Science and
- 757 Food Safety, 18(5), 1533-1549, doi:10.1111/1541-4337.12476.
- 758 Zhang, M., Sun, J., & Chen, P. (2017). Development of a Comprehensive Flavonoid Analysis
- 759 Computational Tool for Ultrahigh-Performance Liquid Chromatography-Diode Array Detection-
- 760 High-Resolution Accurate Mass-Mass Spectrometry Data. *Anal Chem*, 89(14), 7388-7397,
- 761 doi:10.1021/acs.analchem.7b00771.
- Zhang, M., Sun, J., & Chen, P. (2015). FlavonQ: An Automated Data Processing Tool for
- 763 Profiling Flavone and Flavonol Glycosides with Ultra-High-Performance Liquid
- 764 Chromatography-Diode Array Detection-High Resolution Accurate Mass-Mass Spectrometry.
- 765 Anal Chem, 87(19), 9974-9981, doi:10.1021/acs.analchem.5b02624.
- Zhang, Z., Kou, X., Fugal, K., & McLaughlin, J. (2004). Comparison of HPLC Methods for
- 767 Determination of Anthocyanins and Anthocyanidins in Bilberry Extracts. *Journal of Agricultural*
- 768 and Food Chemistry, 52(4), 688-691, doi:10.1021/jf034596w.
- 769 Zhu, M., Zheng, X., Shu, Q., Li, H., Zhong, P., Zhang, H., Xu, Y., Wang, L., & Wang, L. (2012).
- 770 Relationship between the Composition of Flavonoids and Flower Colors Variation in Tropical
- 771 Water Lily (Nymphaea) Cultivars. *PLOS ONE*, 7(4), e34335.